

Intramolecular Homolytic Substitution Chemistry: An *ab Initio* Study of 1,*n*-Chalcogenyl Group Transfer and Cyclization Reactions in Some ω -Chalcogenylalkyl Radicals

Carl H. Schiesser* and Lisa M. Wild

School of Chemistry, The University of Melbourne, Parkville, Victoria 3052, Australia

Received July 14, 1998

Ab initio calculations using a pseudopotential (DZP) basis set and with the inclusion of electron correlation (MP2) predict that intramolecular homolytic substitution at the chalcogen atom in the 4-chalcogenyl-1-butyl (**4**), 5-chalcogenyl-1-pentyl (**5**), 6-chalcogenyl-1-hexyl (**6**), and 7-chalcogenyl-1-heptyl radicals (**7**) proceeds preferentially with the degenerate translocation of the chalcogen-containing moiety for radicals **6** and **7** and with ring closure in the case of the lower homologues (**4**, **5**). All reactions involving homolytic substitution at the tellurium atom are predicted to proceed with the involvement of [9-Te-3] hypervalent intermediates, while the analogous reactions involving sulfur and selenium are calculated to proceed without the involvement of intermediates at all levels of theory, except during the 1,6-translocation of selanyl in which a shallow local minimum was located on the potential-energy surface at the MP2/DZP level of theory. Energy barriers for ring-closure reactions of between 48.4 (cyclization of **4**: E = Te) and 162.6 kJ·mol⁻¹ (cyclization of **5**: E = S) are calculated and are expected to decrease significantly with the inclusion of better leaving groups. Energy barriers for 1,*n*-translocation reactions of between 62.8 (1,7-tellanyl transfer) and 139.3 kJ·mol⁻¹ (1,5-sulfanyl transfer) are predicted at the MP2/DZP level of theory; these high energy barriers are presumably a consequence of unfavorable factors associated with ring size and long carbon–chalcogen separations in transition states and intermediates (**9**–**13**) which lead to significant deviations from the ideal arrangement of attacking and leaving radicals preferred in homolytic substitution reactions at chalcogen. The dependence of transition-state energy on attack angle at chalcogen has been explored for the attack of methyl radical at methanethiol. Attack angles of around 110° are calculated to lead to increases in the energy barrier of about 140 kJ·mol⁻¹ when compared with the preferred (159.5°) arrangement of attacking and leaving groups. The mechanistic implications of these predictions are discussed.

Introduction

It is now well recognized that free-radical chemistry is an important tool in the chemical armory available to the synthetic chemist.^{1,2} Apart from the fundamental and increasingly popular role that inter- and intramolecular homolytic addition chemistry plays in the construction of bonds to carbon,¹ homolytic substitution chemistry is fast becoming one of the methods of choice in synthetic strategies which require the formation of bonds to heteroatoms.²

While there are numerous examples involving the use of intermolecular homolytic substitution reactions in synthetic application,³ there are considerably fewer reports detailing the use of the analogous intramolecular

chemistry.² Intramolecular reactions in which the leaving radical is ejected from the molecule of interest usually result in the formation of higher heterocycles. Indeed, homolytic substitution has been effectively used for the construction of sulfur-,⁴ selenium-⁵ and tellurium-containing⁶ rings as well as silacycloalkanes.⁷

(1) Giese, B., *Radicals in Organic Synthesis: Formation of Carbon–Carbon Bonds*; Pergamon Press: Oxford, 1986 and references therein. Regitz, M.; Giese, B. *Radical, Houben-Weyl Methoden der Organischen Chemie*; Georg Thieme: Stuttgart, 1989; Vol. E 19a. Perkins, M. J. *Radical Chemistry*; Ellis-Horwood: New York, 1994. Beckwith, A. L. J.; Ingold, K. U. In *Rearrangements in Ground and Excited States*; 1980; de Mayo, P., Ed.; Academic Press: New York, Vol. 1, p 161. Beckwith, A. L. J. *Tetrahedron* **1981**, *37*, 3073. Ramaiah, M. *Tetrahedron* **1987**, *43*, 3541. Curran, D. P. *Synthesis* **1988**, 417. Porter, N. A.; Giese, B.; Curran, D. P. *Acc. Chem. Res.* **1991**, *24*, 296. Bowman, W. R. In *Organic Reaction Mechanisms*; Knipe, A. C., Watts, W. E., Eds.; Wiley: New York, 1992; Chapter 3, p 73. Newcomb, M. *Tetrahedron* **1993**, *49*, 1151. Beckwith, A. L. J. *J. Chem. Soc. Rev.* **1993**, *22*, 143. Beckwith, A. J. L.; Crich, D.; Duggan, P. J.; Yao, Q. *Chem. Rev.* **1997**, *97*, 3273.

(2) Schiesser, C. H.; Wild, L. M. *Tetrahedron* **1996**, *52*, 13256 and references therein. Walton, J. *Acc. Chem. Res.* **1998**, *31*, 99 and references therein.

(3) Curran, D. P. *Synthesis* **1988**, 489. Curran, D. P.; Eichenberger, E.; Collis, M.; Roepel, M. G.; Thoma, G. *J. Am. Chem. Soc.* **1994**, *116*, 4279. Byers, J. H.; Gleason, T. G.; Knight, K. S. *J. Chem. Soc., Chem. Commun.* **1991**, 354. Crich, D.; Chen, C.; Hwang, J.-T.; Yuan, H.; Papadatos, A.; Walter, R. I. *J. Am. Chem. Soc.* **1994**, *116*, 8937. Barton, D. H. R.; Ozbalik, N.; Sarma, J. C. *Tetrahedron Lett.* **1988**, *29*, 6581. Barton, D. H. R.; Ramesh, M. *J. Am. Chem. Soc.* **1990**, *112*, 891. Engman, L.; Gupta, V. *J. Org. Chem.* **1997**, *62*, 157. Lucas, M. A.; Schiesser, C. H. *J. Org. Chem.* **1996**, *61*, 5754.

(4) Kampmeier, J. A.; Evans, T. R. *J. Am. Chem. Soc.* **1966**, *88*, 4096. Benati, L.; Montevicchi, P. C.; Tundo, A.; Zanardi, G. *J. Chem. Soc., Perkin Trans. 1* **1974**, 1272. Lawson, A. J. *Phosphorus Sulfur and the Related Elements* **1982**, *12*, 357. Beckwith, A. L. J.; Boate, D. R. *J. Org. Chem.* **1988**, *53*, 4339. Beckwith, A. L. J.; Boate, D. R. *J. Chem. Soc. Chem. Commun.* **1986**, 189. Beckwith, A. L. J.; Duggan, S. A. M. *J. Chem. Soc., Perkin Trans. 2* **1994**, 1509. Franz, J. A.; Roberts, D. H.; Ferris, K. F. *J. Org. Chem.* **1987**, *52*, 2256. John, D. I.; Tyrrell, N. D.; Thomas, E. J. *J. Chem. Soc., Chem. Commun.* **1981**, 901. Tada, M.; Nakagiri, H. *Tetrahedron Lett.* **1992**, *33*, 6657. Tada, M.; Uetaka, T.; Matsumoto, M. *J. Chem. Soc., Chem. Commun.* **1990**, 1408.

(5) Schiesser, C. H.; Sutej, K. *J. Chem. Soc., Chem. Commun.* **1992**, 57. Schiesser, C. H.; Sutej, K. *Tetrahedron Lett.* **1992**, *33*, 5137. Lyons, J. E.; Schiesser, C. H.; Sutej, K. *J. Org. Chem.* **1993**, *58*, 5632. Benjamin, L. J.; Schiesser, C. H.; Sutej, K. *Tetrahedron* **1993**, *49*, 2557. Fong, M. C.; Schiesser, C. H. *Tetrahedron Lett.* **1993**, *34*, 4347. (b) Fong, M. C.; Schiesser, C. H. *Tetrahedron Lett.* **1995**, *36*, 7329. Fong, M. C.; Schiesser, C. H. *J. Org. Chem.* **1997**, *62*, 3103. Lucas, M. A.; Schiesser, C. H. *J. Org. Chem.* **1998**, *63*, 3032.

(6) Laws, M. J.; Schiesser, C. H. *Tetrahedron Lett.* **1997**, *38*, 8429.

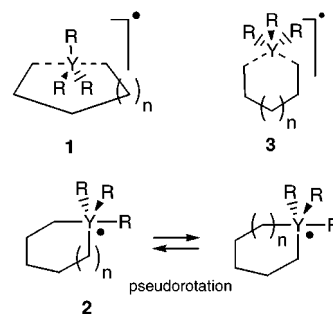
Intramolecular translocation chemistry in molecules containing halo, phenylthio, trialkylsilyl, germlyl, and stannyl moieties is representative of a homolytic substitution process in which the attacking and leaving radical form part of the same molecule.² In addition to several reports involving 1,2-silyl and germlyl shifts,⁸ intramolecular homolytic group transfers involving silicon, germanium, and tin have been put to good use by Davies and co-workers⁹ as well as by Kim and his associates.¹⁰ There also appear to be several early reports of 1,2-migrations of halogen,¹¹ the Nesmeyanov rearrangement¹² typifying this chemistry.

Apart from the 1,2-translocation chemistry mentioned above, and despite efforts in this area,¹³ we are aware of only one example involving intramolecular homolytic translocation of a sulfur-containing group¹⁴ and are unaware of any examples involving selenium, tellurium, or halogen.² The question of why so few intramolecular transfers involving halogen- and chalcogen-containing groups have been reported is likely to be a consequence of the mechanism of homolytic substitution at these heteroatoms.¹⁵

Recently, we published a comprehensive ab initio study of 1,*n*-halogen atom transfers in a series of ω -haloalkyl radicals and concluded that these translocations are unlikely to be synthetically useful mainly because of the strain engendered in the cyclic transition states associated with these reactions as a result of the bending of the C–X–C angle away from the preferred collinear arrangement.¹⁶

Intramolecular homolytic substitution by a radical at a group (Y) can proceed via either a transition state (**1**) in which the attacking and leaving groups adopt a collinear (or nearly so) arrangement resulting in Walden inversion or with the involvement of a hypervalent intermediate (**2**) which may or may not undergo pseudo-

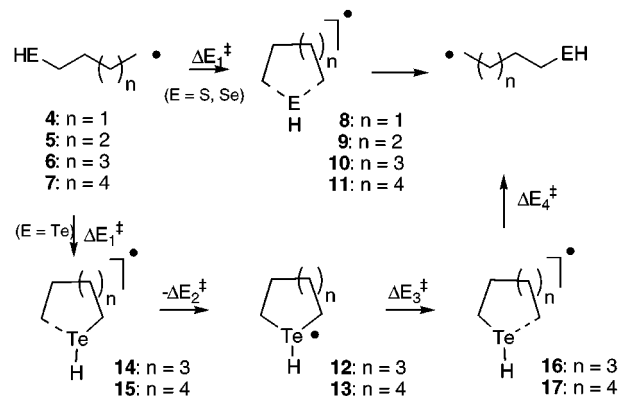
rotation prior to dissociation.¹⁵ The possibility of a third *front-side* mechanism involving transition state **3** is also possible.



Ab initio calculations performed in our laboratories (MP2/DZP, QCISD/DZP) suggest that intermolecular homolytic substitutions by alkyl radicals at the chalcogen atom in alkanethiols and selenols proceed via transition states in which the attacking and leaving radicals adopt arrangements in which C–E–C angles generally fall in the range 150–180°, while reactions at tellurium are predicted to involve [9-Te-3] hypervalent intermediates.¹⁷

To provide further insight into the mechanistic details of intramolecular homolytic substitution chemistry, we began to explore 1,*n*-chalcogenyl transfer and ring-closure reactions involving ω -chalcogenylalkyl radicals (**4**–**7**) (Scheme 1) through the use of ab initio molecular-orbital

Scheme 1



calculations. We now report that intramolecular homolytic substitutions at chalcogen are predicted to preferentially form five- and six-membered heterocycles for reactions involving the lower homologous radicals (**4**, **5**); MP2/DZP calculations predict energy barriers of between about 50 and 96 kJ·mol⁻¹. In comparison, the larger systems (**6**, **7**) are predicted to preferentially become involved in translocation chemistry, with barriers calculated to lie in the range 63–139 kJ·mol⁻¹ at the same level of theory.

Methods

Ab initio molecular orbital calculations were performed on Sun SparcServer 10/512, DEC AlphaStation 400 4/233, Cray Y-MP4E/364, Cray J916 or DEC 8400 computers using the Gaussian 94¹⁸ system of programs. Wherever possible, geometry optimizations were performed using standard gradient

(7) Kulicke, K. J.; Chatgialiloglu, C.; Kopping, B.; Giese, B. *Helv. Chim. Acta* **1992**, *75*, 935.

(8) Pitt, C. G.; Fowler, M. S. *J. Am. Chem. Soc.* **1968**, *90*, 1928. West, R.; Boudjouk, P. *J. Am. Chem. Soc.* **1973**, *95*, 3983. Harris, J. M.; MacInnes, I.; Walton, J. C.; Maillard, B. *J. Organomet. Chem.* **1991**, *403*, C25. Harris, J. M.; Walton, J. C.; Maillard, B.; Grellet, S.; Picard, J.-P. *J. Chem. Soc., Perkin Trans. 2* **1993**, 2119. Roberts, B. P.; Vazquez-Persaud, A. R. *J. Chem. Soc., Perkin Trans. 2* **1995**, 1087. Alberti, A.; Hudson, A. *Chem. Phys. Lett.* **1977**, *48*, 331. Prokofev, A. I.; Prokofeva, T. I.; Belostotskaya, I. S.; Bubnov, N. N.; Solodovnikov, S. P.; Ershov, V. V.; Kabachnik, M. I. *Tetrahedron* **1979**, *35*, 2471. Barker, P. J.; Davies, A. G.; Hawari, J. A.-A.; Tse, M.-W. *J. Chem. Soc., Perkin Trans. 2* **1980**, 1488. Davies, A. G.; Hawari, J. A.-A. *J. Organomet. Chem.* **1983**, *251*, 53. Dalton, J. C.; Bourque, R. A. *J. Am. Chem. Soc.* **1981**, *103*, 699. Tsai, Y.-M.; Cherng, C.-D. *Tetrahedron Lett.* **1991**, *32*, 3515.

(9) Davies, A. G.; Tse, M.-W. *J. Organomet. Chem.* **1978**, *155*, 25.

(10) Kim, S.; Koh, J. S. *J. Chem. Soc., Chem. Commun.* **1992**, 1377. Kim, S.; Lee, S.; Koh, J. S. *J. Am. Chem. Soc.* **1991**, *113*, 5106. Kim, S.; Lim, K. M. *J. Chem. Soc., Chem. Commun.* **1993**, 1152. Kim, S.; Lim, K. M. *Tetrahedron Lett.* **1993**, *34*, 4851. Kim, S.; Do, J. Y.; Lim, K. M. *J. Chem. Soc., Perkin Trans. 1* **1994**, 2517. Kim, S.; Do, J. Y.; Lim, K. M. *Chem. Lett.* **1996**, 669.

(11) Beckwith, A. L. J.; Ingold, K. U. in *Rearrangements in Ground and Excited States*; de Mayo, P., Ed.; Academic Press: New York, 1980; Vol. 1, p 248 and references therein. Kaplan, L. *Bridged Free Radicals*; Marcel Dekker Inc.: New York, 1972.

(12) Nesmeyanov, A. N.; Freidlina, R. Kh.; Firstov, V. I. *Izv. Akad. Nauk. SSSR, Otd. Khim., Nauk.* **1951**, 505. Nesmeyanov, A. N.; Freidlina, R. Kh.; Zakharkin, L. I. *Dokl. Akad. Nauk. SSSR*, **1951**, *81*, 199. Urry, W. H.; Eiszner, J. R. *J. Am. Chem. Soc.* **1952**, *74*, 5822.

(13) Kampmeier, J. A.; Jordan, R. B.; Liu, M. S.; Yamanaka, H.; Bishop, D. J. In *Organic Free Radicals*; Pryor, W. A., Ed.; American Chemical Society: Washington, D.C., **1978**; pp 275–289.

(14) Fong, M. C.; Schuesser, C. H. *Aust. J. Chem.* **1992**, *45*, 475.

(15) Volatron, F.; Demolliens, A.; Lefour, J.-M.; Eisenstein, O. *Chem. Phys. Lett.* **1986**, *130*, 419. Volatron, F. *J. Mol. Struct.: THEOCHEM* **1989**, *186*, 167.

(16) Schuesser, C. H.; Wild, L. M. *J. Org. Chem.* **1998**, *63*, 670.

(17) Schuesser, C. H.; Smart, B. A. *Tetrahedron* **1995**, *51*, 6051. See correction in the following: Schuesser, C. H.; Smart, B. A.; Tran, T.-A. *Tetrahedron* **1995**, *51*, 10651.

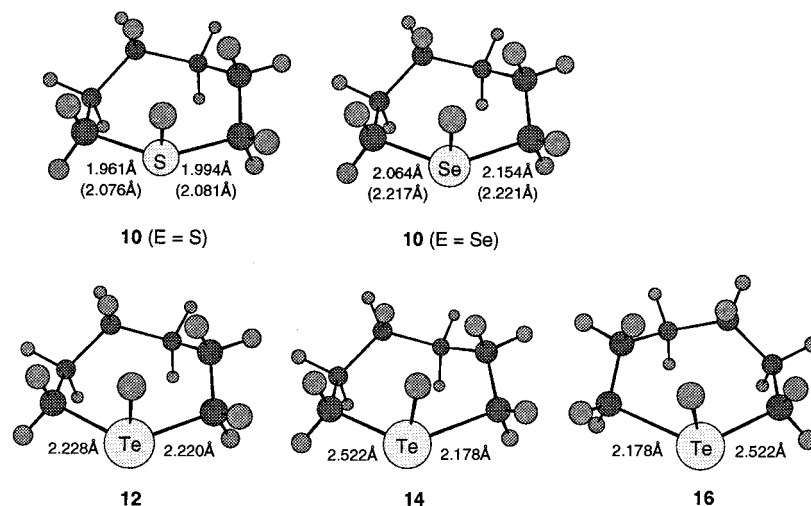


Figure 1. MP2/DZP calculated transition structures (**10**, **14**, **16**) and intermediate (**12**) involved in 1,6-chalcogenyl transfer in 6-chalcogenyl-1-hexyl radicals (**6**) (UHF/DZP data in parentheses).

techniques at the SCF and MP2 levels of theory using the 3-21G^(*) and a (valence) double- ζ pseudopotential basis set (DZP). Full details of the DZP basis have been published elsewhere.^{17,19} For some of the smaller systems, QCISD calculations are also included. The nature of all structures was verified by vibrational-frequency analysis at the UHF and MP2 levels of theory. Calculated energies and optimized geometries of all structures in this study are contained in the Supporting Information except for those for the methyl radical and the methanechalcogenols which have been published previously.¹⁷

Results and Discussion

Homolytic Translocations in 6-Chalcogenyl-1-hexyl and 7-Chalcogenyl-1-heptyl Radicals (6, 7). Reaction profiles for intramolecular homolytic attack at the chalcogen atom in 6-chalcogenyl-1-hexyl and 7-chalcogenyl-1-heptyl radicals (**6**, **7**) resulting in translocation of the chalcogen-containing moiety were explored at the UHF/3-21G^(*), UHF/DZP, and MP2/DZP levels of theory. Transition states (**10** and **11**) of C_1 symmetry were located for reactions involving attack at sulfur and selenium at all levels of theory employed in this study, while the analogous tellurium-containing structures **12** and **13** proved, as expected from previous intermolecular calculations, to correspond to local minima on the C₆H₁₃-Te and C₇H₁₅Te potential-energy surfaces at the MP2/DZP level of theory, connected to the starting and rearranged forms of radicals **6** and **7** (E = Te) by transition states **14** – **17**. At no level of theory could any ring-closure transition state be located in these systems. Calculated transition-state geometries are displayed in

Figures 1 and 2, while calculated reaction energy barriers ($\Delta E_1^\ddagger - \Delta E_4^\ddagger$; Scheme 1), asymmetric vibrational frequencies, and important geometric features of structures **10** and **12** are listed in Table 1.

Inspection of Table 1 reveals that the transition state **10** (E = S) associated with 1,6-transfer of sulfanyl is calculated to lie some 183.7 kJ·mol⁻¹ above the reactant **6**, (E = S) in energy using UHF/3-21G^(*). The energy barrier (ΔE_1^\ddagger) is predicted to increase somewhat with the better basis set to a value of 205.3 kJ·mol⁻¹ (UHF/DZP). Inclusion of electron correlation in these calculations serves to reduce this energy barrier to 121.7 kJ·mol⁻¹ at the MP2/DZP level of theory.

Similar trends are predicted for 1,6-transfers involving selanyl with calculated barriers of 150.2 (UHF/3-21G^(*)), 184.5 (UHF/DZP), and 104.0 kJ·mol⁻¹ (MP2/DZP) for the degenerate rearrangement of **6** (E = Se). In the reaction involving 1,6-transfer of tellanyl, MP2/DZP calculations predict that **12** corresponds to a [9-Te-3] intermediate which lies 68.3 kJ·mol⁻¹ above the starting radical **6** (E = Te) in energy with barriers (ΔE_2^\ddagger , ΔE_3^\ddagger) of 9.8 and 10.0 kJ·mol⁻¹ to dissociation.

Very similar reaction profiles are calculated for the degenerate rearrangements involving the 7-chalcogenyl-1-heptyl radicals **7**; structure **11** proved to correspond to a transition state at all levels of theory for translocations involving sulfanyl and selanyl, while the reaction involving tellurium is predicted to involve a [9-Te-3] intermediate (**13**). Energy barriers (ΔE_1^\ddagger) of 170.0, 194.9, and 112.9 kJ·mol⁻¹ are calculated at the UHF/3-21G^(*), UHF/DZP, and MP2/DZP levels of theory, respectively, for **7** (E = S), while values of 136.0 (UHF/3-21G^(*)), 171.3 (UHF/DZP), and 92.5 (MP2/DZP) kJ·mol⁻¹ are calculated for **7** (E = Se). MP2/DZP calculations predict that **13** lies some 57.8 kJ·mol⁻¹ above **7** (E = Te) with barriers (ΔE_2^\ddagger , ΔE_3^\ddagger) of 5.0 and 5.2 kJ·mol⁻¹ to dissociation via transition states **15** and **17**, respectively.

It should be noted that both C_s and C_1 transition states were located at the UHF/3-21G^(*) level of theory for the rearrangement of **7** (E = S). As the C_s structure proved to lie 24.2 kJ·mol⁻¹ above the C_1 structure (**11**, E = S) in energy, and given the sheer size of calculations involving **7**, we chose not to explore further reactions involving any C_s structure involved in the rearrangement of **7**.

(18) Frisch, M. J.; Trucks, G. W.; Schlegel, H. B.; Gill, P. M. W.; Johnson, B. G.; Robb, M. A.; Cheeseman, J. R.; Keith, T.; Petersson, G. A.; Montgomery, J. A.; Raghavachari, K.; Al-Laham, M. A.; Zakrzewski, V. G.; Ortiz, J. V.; Foresman, J. B.; Peng, C. Y.; Ayala, P. Y.; Chen, W.; Wong, M. W.; Andres, J. L.; Replogle, E. S.; Gomperts, R.; Martin, R. L.; Fox, D. J.; Binkley, J. S.; Defrees, D. J.; Baker, J.; Stewart, J. J. P.; Head-Gordon, M.; Gonzalez, C.; Pople, J. A. *Gaussian 94*, Revision B.3, Gaussian Inc., Pittsburgh, PA, 1995.

(19) Schiesser, C. H.; Smart, B. A. *J. Comput. Chem.* **1995**, *16*, 1055. Styles, M. L.; Wild, L. M. *J. Chem. Soc., Perkin Trans. 2* **1996**, 2257. Dakternieks, D.; Henry, D. J.; Schiesser, C. H. *J. Chem. Soc., Perkin Trans. 2* **1997**, 1665. Schiesser, C. H.; Styles, M. L. *J. Chem. Soc., Perkin Trans. 2* **1997**, 2335. Schiesser, C. H.; Skidmore, M. A. *J. Organomet. Chem.* **1998**, *552*, 145. Dakternieks, D.; Henry, D. J.; Schiesser, C. H. *J. Chem. Soc., Perkin Trans. 2* **1998**, 591. Dakternieks, D.; Henry, D. J.; Schiesser, C. H. *Organometallics* **1998**, *17*, 1079.

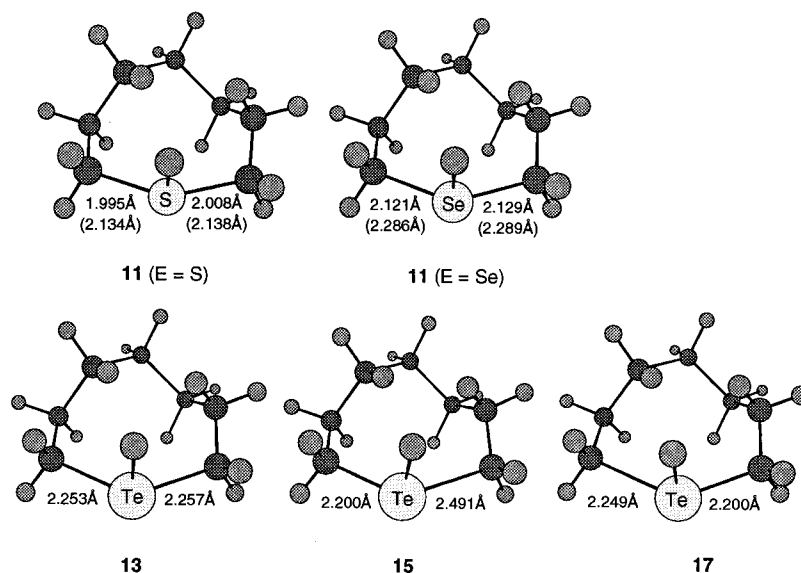


Figure 2. MP2/DZP calculated transition structures (**11**, **15**, **17**) and intermediate (**13**) involved in 1,7-chalcogenyl transfer in 7-chalcogenyl-1-heptyl radicals (**7**) (UHF/DZP data in parentheses).

Table 1. Calculated Energy Barriers^a ($\Delta E_1^\ddagger - \Delta E_4^\ddagger$; Scheme 1) for 1,6- and 1,7-Chalcogenyl Transfer Reactions in ω -Chalcogenyl-1-alkyl Radicals (**6** and **7**) and the Corresponding Asymmetric Stretching Frequency^b (ν) and Important Geometric Parameters (r_{C-E} , r_{E-H} , θ)^c (Figures 1 and 2) of the Cyclic Structures **10**–**13**

structure		ΔE_1^\ddagger	ΔE_2^\ddagger	ΔE_3^\ddagger	ΔE_4^\ddagger	ν	r_{C-E}	r_{E-H}	θ
10 (E = S)	UHF/3-21G ^(*)	183.7 (189.5)				696i	2.095	2.100	139.4
	UHF/DZP	205.3 (209.9)				729i	2.076	2.081	137.6
	MP2/DZP	121.7				252i	1.961	1.994	137.3
10 (E = Se)	UHF/3-21G ^(*)	150.2 (157.8)				497i	2.184	2.189	135.2
	UHF/DZP	184.5 (189.4)				545i	2.217	2.221	132.0
	MP2/DZP	104.0				170i	2.064	2.154	132.3
12	MP2/DZP	78.1	9.8	10.0	78.3	81	2.228	2.220	122.7
11 (E = S)	UHF/3-21G ^(*)	170.0 (176.9)				676i	2.145	2.149	146.4
	UHF/DZP	194.9				711i	2.134	2.138	145.9
	MP2/DZP	112.9				366i	1.995	2.008	145.4
11 (E = Se)	UHF/3-21G ^(*)	136.0 (144.1)				501i	2.227	2.231	141.8
	UHF/DZP	171.3				522i	2.286	2.289	139.3
	MP2/DZP	92.5				198i	2.121	2.129	139.5
13	MP2/DZP	62.8	5.0	5.2	63.0	119	2.253	2.257	130.8

^a Energies in $\text{kJ}\cdot\text{mol}^{-1}$ (zero-point corrected data appear in parentheses where available). ^b Frequencies in cm^{-1} . ^c Distances in Å, angles in degrees.

These data are to be compared with the previous calculations for the analogous halogen-translocation chemistry.¹⁶ Barriers of 170.9 (Cl), 149.2 (Br), and 136.0 (I) $\text{kJ}\cdot\text{mol}^{-1}$ are calculated at the MP2/DZP level of theory for 1,6-translocations of a halogen, while the analogous 1,7-transfers are predicted to proceed with barriers of 163.5 (Cl), 137.9 (Br), and 120.0 (I) $\text{kJ}\cdot\text{mol}^{-1}$ at the same level of theory. It is clear that this study predicts 1,6- and 1,7-translocations of chalcogenyl to be more facile than the analogous reactions involving a halogen. It is noteworthy that transition states of both C_s and C_2 symmetry were located for each 1,7-halogen translocation reaction with the C_s structures proving to be of lower energy.

Inspection of Table 1 together with Figures 1 and 2 reveals some interesting geometrical features which may help in our understanding of the high barriers associated with the intramolecular chalcogenyl transfer reactions in this study. The MP2/DZP carbon–chalcogen distances in the structures (**10**) are calculated to be about 1.97 (S) and 2.10 (Se) Å and are calculated to be about 2.23 (Te) Å in **12**, while the similar distances in **11** and **13** are

calculated to be about 2.01 (S), 2.13 (Se), and 2.26 (Te) Å at the same level of theory. These large separations lead to significant deviations from the ideal arrangement of attacking and leaving groups.¹⁷ As was observed in the analogous halogen series, the C–E–C angle becomes increasingly more severe as the C–E distance increases; MP2/DZP calculations predict angles of 137° (S) and 132° (Se) in structures **10** and 123° (Te) in **12**, while values of 145° (S), 140° (Se), and 131° (Te) are calculated for structures **11** and **13**. We believe these deviations to be responsible for the high-energy barriers predicted to be associated with these reactions (vide infra). It is no surprise, therefore, that 1,7-translocations of chalcogenyl, with larger C–E–C angles in structures **11** and **13** than in the corresponding 1,6-translocation transition state **10** or intermediate **12**, are predicted to have smaller energy barriers for translocation.

Reactions of 5-Chalcogenyl-1-pentyl Radicals (5). Despite considerable searching of the $C_5H_{11}E$ (E = S, Se, Te) potential-energy surfaces using UHF/3-21G^(*), UHF/DZP, and MP2/DZP methods, C_s symmetric structures **9** could only be located for reactions involving transfer of

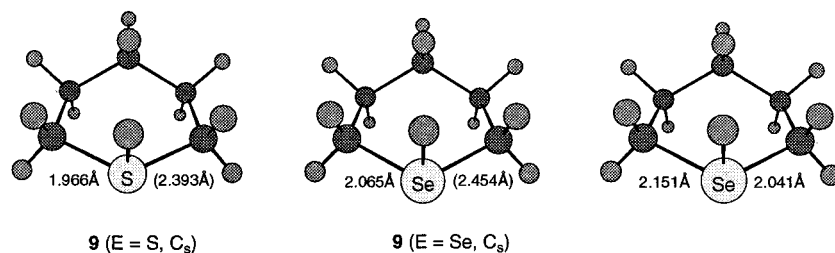
**9** (E = S, C_s)**9** (E = Se, C_s)

Figure 3. UHF/3-21G^(*) and MP2/DZP calculated transition structures (**9**, E = S) involved in 1,5-sulfanyl translocation, UHF/3-21G^(*) calculated transition state (**9**, E = Se) and MP2/DZP calculated intermediate (**9**, E = Se) involved in 1,5-selenyl translocation, and the MP2/DZP calculated transition state (right) for the formation of intermediate (**9**, E = Se) (UHF/3-21G^(*) data in parentheses).

Table 2. Calculated Energy Barriers^a(ΔE_1^\ddagger , Scheme 1) for 1,5-Chalcogenyl Transfer Reactions in 5-Chalcogenyl-1-pentyl Radicals (**5**) and the Corresponding Asymmetric Stretching Frequency^b(ν) and Important Geometric Parameters (r , θ)^c (Figure 3) of the Cyclic Structures **9**

structure	ΔE_1^\ddagger	$\Delta E_{\text{well}}^\ddagger$	ν	r	θ
9 (E = S)	UHF/3-21G ^(*)	223.5 (215.7)	672i	2.393	114.5
	MP2/DZP	139.3	210i	1.966	121.3
9 (E = Se)	UHF/3-21G ^(*)	200.0 (193.9)	627i	2.454	124.4
	MP2/DZP ^d	118.4 ^e	0.7	150	2.065

^aEnergies in kJ·mol⁻¹ (zero-point corrected data appear in parentheses where available). ^bFrequencies in cm⁻¹. ^cDistances in Å, angles in degrees. ^dStructure **9** (E = Se) corresponds to an intermediate at MP2/DZP. ^eEnergy barrier for the formation of **9** (E = Se).

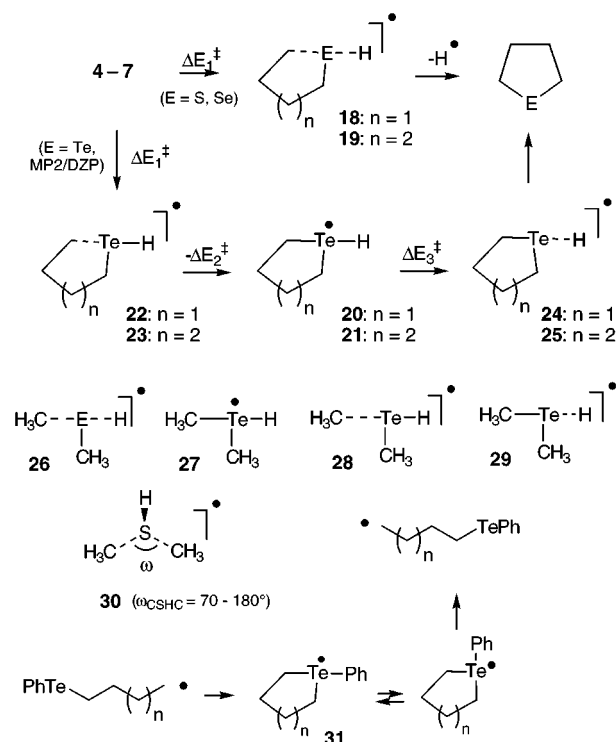
sulfanyl and selenyl at the UHF/3-21G^(*) and MP2/DZP levels of theory. Structures **9** proved to correspond to the transition states for translocation of the chalcogen-containing group except for **9** (E = Se) which proved to correspond to a local minimum at the MP2/DZP level of theory. This is a significant result as it represents the first example of a [9-Se-3] intermediate located in any ab initio calculation involving attack of alkyl radical at a selenium atom. The energy barrier to dissociation of **9** (E = Se) is calculated to be only 0.7 kJ·mol⁻¹ at the MP2/DZP level of theory; clearly, then, this structure is more likely to behave like a transition state than a hypervalent intermediate.

Energy barriers (ΔE_1^\ddagger ; Scheme 1) able to be determined for the reactions in question are listed in Table 2 together with the significant geometric features and the important asymmetric vibrational frequencies of structures **9**; calculated structures are displayed in Figure 3.

Inspection of Table 2 reveals that the transition state **9** (X = S) lies some 139–224 kJ·mol⁻¹ above the reactant **5** (E = S) in energy, depending on the level of theory. At the highest level (MP2/DZP) this barrier (139.3 kJ·mol⁻¹) is calculated to be some 17.6 and 26.4 kJ·mol⁻¹ higher than the analogous 1,6- and 1,7-translocation in **6** and **7** (E = S), respectively; this difference is predicted to be 39.8 and 52.8 kJ·mol⁻¹, respectively, using UHF/3-21G^(*). This trend in energy barriers is almost certainly the result of the even greater deviation from the preferred arrangement of attacking and leaving groups at sulfur in structure **9**, (E = S) when compared to **10** and **11** (E = S). The C–S–C angle in the six-membered transition state (**9**) is calculated to be 121.3° (MP2/DZP), which is significantly smaller than the values of 137.3° and 145.4° calculated for the analogous seven- and eight-membered structures, respectively, at the same level of theory. It is interesting to note that the MP2/DZP calculated C–S distance in **9** (E = S) of 1.966 Å is very similar to those

calculated for **10** and **11** (E = S) at the same level of theory and that the C–Se–C angle in intermediate **9** (E = Se) is calculated to be 114.3°, once again, significantly smaller than the corresponding angles in transition states **10** and **11** (E = Se). Not surprisingly, 1,5-translocation of selenyl is also predicted to require significantly more energy than the similar 1,6- and 1,7-translocations.

While pathways for direct 1,5-translocations of sulfanyl- and selenyl-containing groups were able to be located, it is significant that no 1,5-translocation pathway was able to be located for the analogous reaction involving tellurium. More significantly, for ring-closure leading to the six-membered heterocycles, structures **19** and **21** were located at every level of theory and for each chalcogen in this study. Not unexpectedly, **19** proved to correspond to transition states in reactions involving sulfur and selenium, while **19** (E = Te) proved to correspond to a transition state at uncorrelated levels of theory.

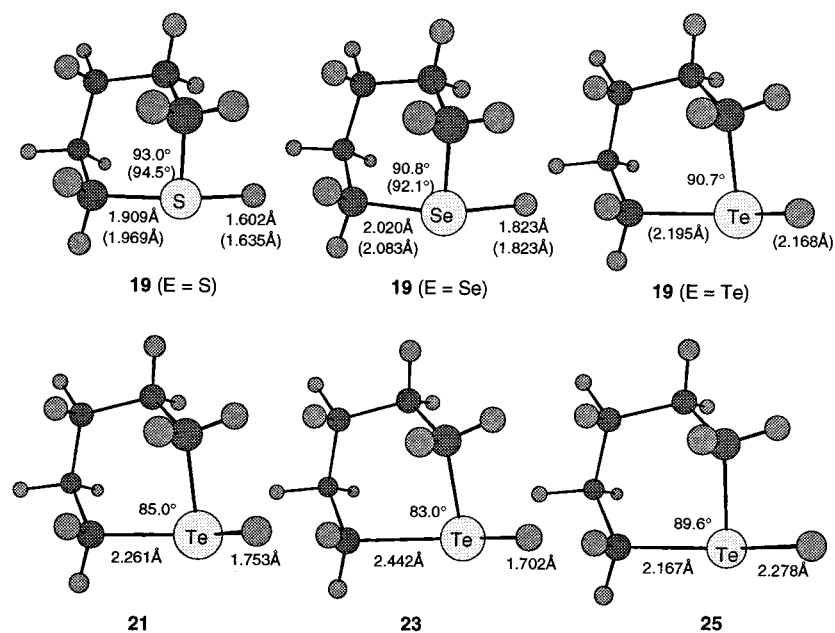
Scheme 2

Energy barriers ($\Delta E_1^\ddagger - \Delta E_3^\ddagger$; Scheme 2) for ring closure of radicals **5** are listed in Table 3, while the MP2/DZP generated structures of the transition states and/or

Table 3. Calculated Energy Barriers^a ($\Delta E_1^\ddagger - \Delta E_3^\ddagger$; Scheme 2) for the Homolytic Ring-closure Reactions of 5-Chalcogenyl-1-pentyl Radicals (**5**) and the Corresponding Asymmetric Stretching Frequency^b (ν) and Important Geometric Parameters (r_{C-E} , r_{E-H})^c (Figure 4) of the Cyclic Structures **19** and **21**

structure		ΔE_1^\ddagger	ΔE_2^\ddagger	ΔE_3^\ddagger	ν	r_{E-H}	r_{E-C}
19 (E = S)	UHF/3-21G ^(*)	144.6 (141.2)			1155i	1.655	2.008
	UHF/DZP	162.6 (159.8)			1054i	1.635	1.969
	MP2/DZP	91.3			627i	1.602	1.909
19 (E = Se)	UHF/3-21G ^(*)	110.1 (109.7)			823i	1.787	2.095
	UHF/DZP	141.1 (139.3)			859i	1.823	2.083
	MP2/DZP	72.0			675i	1.823	2.020
19 (E = Te)	UHF/3-21G ^(*)	85.7 (86.1)	2.8 (0.7)	19.5	667i	2.198	2.216
	UHF/DZP	117.5 (116.8)			672i	2.168	2.195
21	UHF/DZP	33.8			122	1.753	2.261

^a Energies in $\text{kJ}\cdot\text{mol}^{-1}$ (zero-point corrected data appear in parentheses where available). ^b Frequencies in cm^{-1} . ^c Distances in \AA .

**Figure 4.** MP2/DZP calculated transition structures (**19**, **23**, **25**) and intermediate (**21**) involved in the homolytic ring closure of 5-chalcogenyl-1-pentyl radicals (**5**) (UHF/DZP data in parentheses).

intermediates (**19**, **21**, **23**, **25**) involved in these reactions are depicted in Figure 4. Comparison of the data presented in Tables 2 and 3 reveals that the ring-closure reactions of radicals **5** (E = S, Se) are at least $48 \text{ kJ}\cdot\text{mol}^{-1}$ more favorable than the corresponding 1,5-translocation reactions with MP2/DZP calculated energy barriers of 91.3 (S) and 72.0 (Se) $\text{kJ}\cdot\text{mol}^{-1}$. This is a significant prediction and is discussed in more detail below.

The cyclization reaction of **5** (E = Te) is calculated to proceed with an energy barrier of $33.8 \text{ kJ}\cdot\text{mol}^{-1}$ for the formation of intermediate **21** at the MP2/DZP level of theory. This intermediate, in turn, is predicted to lie only $2.8 \text{ kJ}\cdot\text{mol}^{-1}$ in energy below the transition state (**23**) for its formation and some $19.5 \text{ kJ}\cdot\text{mol}^{-1}$ in energy below the transition state (**25**) for expulsion of a hydrogen atom. When a zero-point energy correction is included, **21** is calculated to be constrained by a barrier of only $0.7 \text{ kJ}\cdot\text{mol}^{-1}$.

These data are to be compared with those obtained for analogous intermolecular reactions. MP2/DZP calculations predict energy barriers of 95.9 (S) and 74.2 (Se) $\text{kJ}\cdot\text{mol}^{-1}$ for the attack of the methyl radical at methanethiol and methaneselenol, respectively, with expulsion of a hydrogen atom. These barriers are calculated to increase to 107.1 and $86.0 \text{ kJ}\cdot\text{mol}^{-1}$ at the QCISD/DZP level of theory, respectively. The MP2/DZP calculated C–E and E–H separations in transition state **26** are

calculated to be 1.892 and 1.614 \AA , respectively, for the reaction involving attack at sulfur, and 2.007 and 1.837 \AA , respectively, for the analogous reaction at selenium. Not only are the energy barriers for both inter- and intramolecular processes very similar, the geometrical arrangements of the reacting centers in the intermolecular transition states (**26**; Figure 5) are also similar to those obtained for the ring-closure of **5** (E = S, Se); inspection of Table 3 reveals values of 1.909 and 1.602 \AA (S) and 2.020 and 1.823 \AA (Se) at the same level of theory, suggesting that the transition states for ring closure are only marginally “earlier” than those involved in the analogous intermolecular reactions.

The intermolecular reaction involving tellurium is, once again, predicted to involve an intermediate (**27**) at the MP2/DZP level of theory and is displayed in Figure 5. The transition state (**28**) for the formation of this intermediate is calculated to lie some $30.5 \text{ kJ}\cdot\text{mol}^{-1}$ in energy above that of the reactants and $4.1 \text{ kJ}\cdot\text{mol}^{-1}$ above that of **27** which, in turn, is constrained by a barrier of $14.1 \text{ kJ}\cdot\text{mol}^{-1}$ to form the dimethyl ditelluride. Once again, the similarities in both energy and geometry of the transition states and intermediate involved in both inter- and intramolecular reactions as calculated at the MP2/DZP level of theory are striking. The implications of these calculated observations are discussed in further detail below.

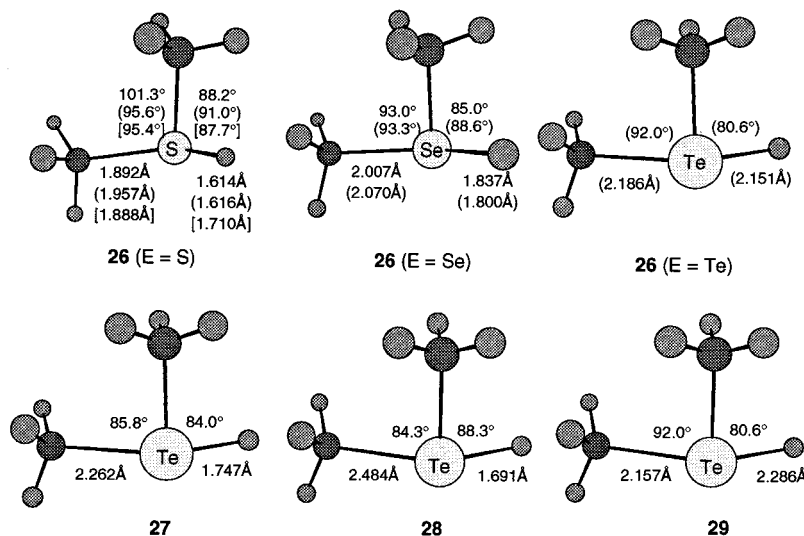


Figure 5. MP2/DZP calculated transition structures (**26**, **28**, **29**) and intermediate (**27**) involved in the intermolecular homolytic substitution of methyl radical at the chalcogen atom in methanechalcogenol with expulsion of hydrogen atom (UHF/DZP data in parentheses) [QCISD/DZP data in brackets].

Table 4. Calculated Energy Barriers^a ($\Delta E_1^\ddagger - \Delta E_3^\ddagger$; Scheme 2) for the Homolytic Ring-Closure Reactions of 4-Chalcogenyl-1-butyl Radicals (**4**) and the Corresponding Asymmetric Stretching Frequency^b (ν) and Important Geometric Parameters (r_{C-E} , r_{E-H})^c (Figure 5) of the Cyclic Structures **18** and **20**

structure		ΔE_1^\ddagger	ΔE_2^\ddagger	ΔE_3^\ddagger	ν	r_{E-H}	r_{E-C}
18 (E = S)	UHF/3-21G ^(c)	142.6 (137.6)			1162i	1.697	2.012
	UHF/DZP	156.7 (152.8)			1054i	1.674	1.966
	MP2/DZP	95.5 (91.9)			837i	1.664	1.905
18 (E = Se)	UHF/3-21G ^(c)	106.8 (104.2)			884i	1.836	2.096
	UHF/DZP	135.3 (131.9)			886i	1.868	2.082
	MP2/DZP	73.0 (69.8)			775i	1.874	2.024
18 (E = Te)	UHF/3-21G ^(c)	78.6 (77.5)	1.3 (-0.5)	25.3 (15.1)	679i	2.240	2.224
	UHF/DZP	111.1 (109.0)			672i	2.217	2.203
20	MP2/DZP	24.4 (29.7)			122	1.736	2.296

^a Energies in $\text{kJ}\cdot\text{mol}^{-1}$ (zero-point corrected data appear in parentheses where available). ^b Frequencies in cm^{-1} . ^c Distances in Å.

Ring Closures of 4-Chalcogenyl-1-butyl Radicals (4). Given the calculated trends discussed above, it came as no surprise that we were unable to locate any transition states or intermediates (**8**) that could possibly be involved in direct translocation of the chalcogen-containing moiety in radicals **4** at any level of theory. Instead, transition states (**18**) for ring closure of **4** were located at each level of theory except for **18** (E = Te) which, as expected, proved to correspond to a local minimum (**20**) at the MP2/DZP level of theory. Energy barriers ($\Delta E_1^\ddagger - \Delta E_3^\ddagger$; Scheme 2) for ring closure of radicals **4** are listed in Table 4, while MP2/DZP generated structures of **18** and **20** as well as the transition states (**22** and **24**) for the formation and dissociation of **20** are displayed in Figure 6.

Inspection of Table 4 and Figure 6 reveals both the structural similarities between the transition states and intermediates (**18** and **20**) involved in the formation of five-membered heterocycles and their higher homologues (**19** and **21**) as well as the striking similarities in energy requirements in both systems. With MP2/DZP calculated energy barriers (ΔE_1^\ddagger) of 95.5 (S) and 73.0 (Se) $\text{kJ}\cdot\text{mol}^{-1}$, it would appear that the formation of tetrahydrothiophene and tetrahydroselenophene, require only 1.0–4.2 $\text{kJ}\cdot\text{mol}^{-1}$ more energy than the similar processes leading to the analogous six-membered ring heterocycles. The similar reaction at tellurium is predicted at MP2/DZP to require 24.4 $\text{kJ}\cdot\text{mol}^{-1}$ for the formation of intermediate **20**, which in turn, lies 1.3 $\text{kJ}\cdot\text{mol}^{-1}$ in energy below the transition

state (**22**) for its formation and 25.3 $\text{kJ}\cdot\text{mol}^{-1}$ below the transition state (**24**) leading to the final product. When zero-point vibrational correction is included, **20** is calculated to become a pseudo-intermediate, lying 0.5 $\text{kJ}\cdot\text{mol}^{-1}$ in energy *above* **22** at the MP2/DZP level of theory.

Strain in Translocation Transition Structures and Intermediates 9–11. As expected on the basis of earlier work involving homolytic substitution at a halogen,¹⁶ the calculations presented in this paper predict homolytic 1,7-chalcogenyl transfer between carbon atoms to be more facile than the analogous 1,6-translocation, which in turn, is more facile than the corresponding 1,5-migration. We believe the reason for this trend lies primarily with the geometric requirements of the transition states and/or intermediates involved in these translocation reactions. As we postulated for reactions involving transfer of a halogen,¹⁶ in each translocation transition structure or intermediate located in this study, the total energy is comprised of several components, of which contributions from C–C–C and C–E–C deformations imposed by the size of the ring and the nature of the heteroatom are likely to be major components. This work, as well as our previous study,¹⁷ predict that attack at a chalcogen by an alkyl radical requires a transition-state or intermediate C–E distance of approximately 2.00 Å (S), 2.13 Å (Se), and 2.26 Å (Te) at the MP2/DZP level of theory. When constrained in a ring by either a 5-, 6-, or 7-carbon chain, necessarily severe C–E–C angles are required. Deviations from the ideal 160–180° arrange-

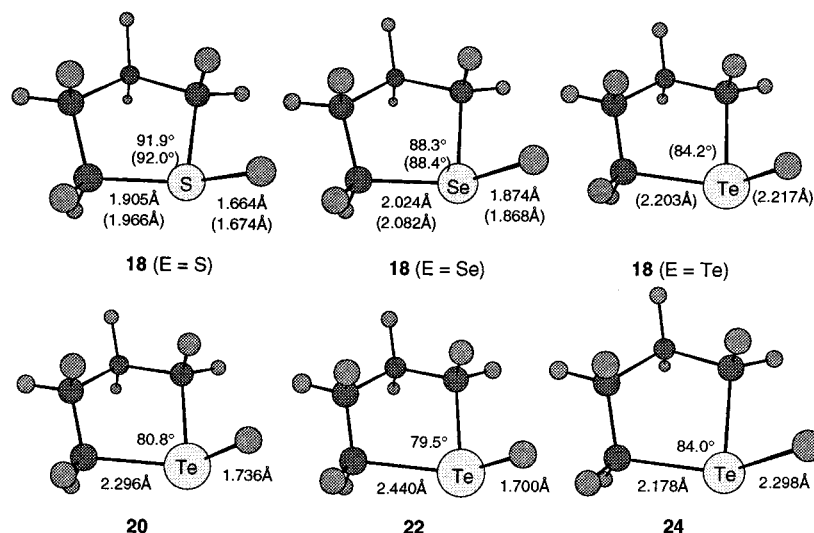


Figure 6. MP2/DZP calculated transition structures (**18**, **22**, **24**) and intermediate (**20**) involved in the homolytic ring closure of 4-chalcogenyl-1-butyl radicals (**4**) (UHF/DZP data in parentheses).

ment for the backside transition state (**1**) would be expected to contribute to the C–E–C deformation energy and therefore to the overall strain energy of the transition state; angles of between 114° and 146° , predicted in this study, together with C–C–C angle strain expected due to the geometry imposed by the chalcogen would certainly be expected to impart considerable strain in structures **9–13**.

Unlike the results of our previous study involving a halogen in which front-side transition states (**2**) were determined to be unlikely,¹⁶ the same need not necessarily be true for reactions involving chalcogen; as the C–E–C angle is reduced, one might expect to realize the transition-state geometry for front-side homolytic substitution. To further investigate this possibility, we examined the effect of variation in the C–S–H–C dihedral angle (ω) on the relative energy of the transition state (**30**) involved in the intermolecular homolytic substitution reaction of methyl radical at the sulfur atom in methanethiol with expulsion of methyl radical at the MP2/DZP level of theory. The MP2/DZP angular energy dependence is displayed in Figure 7. Inspection of Figure 7 reveals that, unlike the analogous profile for homolytic substitution at chlorine (Figure 4, reference 16), which shows a gradual increase in energy of over $100 \text{ kJ}\cdot\text{mol}^{-1}$ in moving from the ideal collinear arrangement (180°) to an attack angle of about 90° , homolytic substitution at sulfur differs in two respects. First, the position of the minimum (the ideal attack angle) on the energy profile is calculated at MP2/DZP to be 159.5° for attack by methyl radical at methanethiol, whereas the similar reaction at chloromethane is predicted to prefer an angle of 180° . Indeed, within the range $150\text{--}210^\circ$, the energy surface changes by less than $2 \text{ kJ}\cdot\text{mol}^{-1}$; clearly, homolytic substitutions at sulfur, and presumably selenium and tellurium also, are predicted to be less sensitive to deviations from collinearity than the analogous reactions at a halogen.

The second important feature clearly evident in Figure 7 is the apparent second “transition state” (**30**, $\omega = 80^\circ$) on the potential-energy surface corresponding to an attack angle of about 80° . This region of the energy surface is calculated to lie some $83 \text{ kJ}\cdot\text{mol}^{-1}$ in energy above the transition state (**30**, $\omega = 159.5^\circ$) corresponding

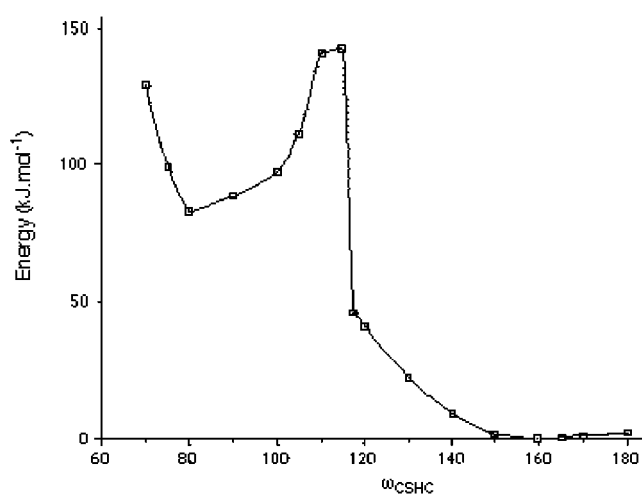


Figure 7. MP2/DZP calculated dependence of the energy of transition state (**30**) on attack angle (ω_{CSHC}) in the reaction of methyl radical at the sulfur atom in methanethiol with expulsion of methyl radical.

to the ideal attack. This second stationary point may represent a front-side-attack pathway and closely resembles that found for front-side homolytic substitution by silyl radical at disilane in which an attack angle of about 80° is also predicted.²⁰ Vibrational-frequency analysis reveals the MP2/DZP generated structure (**30**, $\omega = 80^\circ$) to be a second-order saddle point with one imaginary frequency (985i) corresponding to translocation of sulfanyl and the other (379i) corresponding to collapse to the (true) transition state **26** (E = S) for homolytic substitution by the back-side mechanism. Clearly then, this study suggests that homolytic substitutions by alkyl radicals at sulfur, and presumably at selenium and tellurium, are unlikely to follow a front-side displacement mechanism.

Notwithstanding the argument presented above, and despite being less sensitive to deviations from the ideal attack trajectory, the calculations presented in this paper

(20) Chatgililoglu, C.; Barbieri, A.; Schiesser, C. H.; Wild, L. M. *J. Am. Chem. Soc.*, submitted for publication.

also suggest that 1,5-, 1,6- and 1,7-translocations of chalcogenyl-containing groups by direct homolytic substitution, with energy barriers of between about 60 and 140 kJ·mol⁻¹, are not synthetically viable.

Mechanistic Requirements for Ring-Closure Reactions of ω -Chalcogenylalkyl Radicals (4–7). One of the striking predictions that comes from this work is that intramolecular homolytic substitutions at chalcogen which result in the formation of five- and six-membered heterocycles proceed with very similar energy requirements for a given heteroatom and that these energy requirements are also very similar to those of the analogous intermolecular reactions. We interpret these results in the following way: first, that consistent with early calculations performed in our laboratories,²¹ homolytic substitution at chalcogen is not significantly affected by the nature of the attacking radical for reactions involving the same leaving group; second, that the formations of five- and six-membered rings through intramolecular homolytic substitution are relatively unaffected by the intervening carbon chain and are therefore relatively strain-free, a reasonable suggestion given that the ideal attack angle is easy to adopt in the transition states and/or intermediates involved in these cyclization reactions and that the substituents on the carbon framework are able to adopt staggered orientations as depicted in Figures 4 and 6. We suggest that where this is not possible, as might be the case when seven- and eight-membered rings are involved, then ring closure becomes significantly less favorable. This suggestion is consistent with the observation that the preparations of tetrahydroselenophene and selenane by intramolecular homolytic substitution of the radical centers in 4-benzylseleno-1-butyl and 5-benzoseleno-1-pentyl radicals, respectively, appear to proceed with equal efficiency under the same conditions, whereas the formation of selenopane from 6-benzoseleno-1-hexyl radical is significantly lower in yield.⁵

(21) Lyons, J. E.; Schiesser, C. H. *J. Organomet. Chem.* **1992**, *437*, 165.

While the data in this study suggest that ring-closure reactions in which the leaving radical is a hydrogen atom are expected to be unfavorable, the introduction of more suitable leaving groups (e.g., benzyl, *tert*-butyl) would be expected to result in substantial reductions in energy barrier to the extent that cyclization would be expected to become a substantial reaction pathway; many successful syntheses involving homolytic substitution have been designed on the basis of this premise.² On the other hand, in the presence of poor leaving radicals such as the phenyl group, these calculations suggest that neither translocation nor ring closure would be expected to be feasible processes unless the reactions in question proceed via hypervalent intermediates in which the substituent plays a role in their stability. Translocations involving phenyltelluride may well meet these criteria. While expulsion of phenyl radical would be an unexpected reaction outcome, one would nevertheless envisage the formation of intermediate **31** which may well lie in a significant energy well. Given sufficient lifetime, radical **31** may well pseudorotate prior to dissociation, the result of which would be the effective translocation of the phenyltelluro group. Unfortunately, calculations of the quality and type presented in this paper involving phenyl substitution are beyond our current resources.

Acknowledgment. The support of the Australian Research Council and the Ormond Supercomputer Facility, a joint venture between the University of Melbourne and the Royal Melbourne Institute of Technology, is gratefully acknowledged.

Supporting Information Available: HF/3-21G(*), HF/DZP, MP2/DZP, and QCISD/DZP, calculated energies and Cartesian coordinates (as appropriate) of optimized structures **4–29** as well as dimethyl sulfide, dimethylselenide, and dimethyltelluride (51 pages). This material is contained in libraries on microfiche, immediately follows this article in the microfilm version of the journal, and can be ordered from the ACS; see any current masthead page for ordering information.

JO981376M